X-ray Diffraction and ^{119}Sn Mössbauer Spectroscopy Study of a New Phase in the Bi_2Se_3−SnSe System: $SnBi_4Se_7$

C. Pérez Vicente* and J. L. Tirado

Laboratorio de Química Inorgánica, Facultad de Ciencias, Universidad de Córdoba, Avda. San Alberto Magno s/n, 14004 Córdoba, Spain

K. Adouby† and J. C. Jumas

Laboratoire de Physicochimie de la Matière Condensée (UMR 5617 CNRS), Place Eugène Bataillon, 34095 Montpellier Cedex 5, France

A. Abba Touré and G. Kra

Laboratoire de Chimie Minérale, Faculté de Sciences et Techniques, Université de Cocody, 22 BP 582, Abidjan, Ivory Coast

Received November 6, 1998

First studies of the ternary system SnSe−Bi_2Se_3 developed in 1960s and 1970s have revealed the existence of a nonstoichiometric trigonal phase with a wide range of compositions. In this study, an almost stoichiometric phase, corresponding to the composition $SnBi_4Se_7$, has been identified and isolated. The structure has been determined by X-ray diffraction and the local environment of Sn atoms analyzed by Mössbauer spectroscopy. This phase has a rhombohedral structure, space group $R\bar{3}m$, with hexagonal lattice parameters $a = 4.1602(5)$ Å and $c = 38.934(3)$ Å. The unit cell contains three slabs, each one composed of seven atomic layers according to the sequence Se−Bi−Se−(Bi,Sn)−Se−Bi−Se. Bismuth atoms partially occupy two sites, 3a (0, 0, 0) and 6c (0, 0, z) with $z = 0.4285$, while tin atoms partially occupy only one site, 3a. Selenium atoms are placed in two different 6c sites, with $z_1 = 0.1350$ and $z_2 = 0.7108$.

Introduction

Ternary chalcogenides of groups 14 and 15 have a large diversity of electronic properties, which arise from the different electronic configurations and polyhedra coordination. Particularly Bi_2Te_3 and its solid solutions with Sb_2Te_3 and Bi_2Se_3 find important applications as thermoelectric materials,[1−6] as in temperature-control devices.[7,8] We are mainly interested in Bi_2Se_3 and the solid solutions with SnSe. The first study of the phase diagram of this system, made by Hirai et al. in 1967, indicates the complete miscibility of both Bi_2Se_3 and SnSe compounds.[9] Later in 1974, Odin et al.[10] reported the existence of a new nonstoichiometric phase with a wide range of homogeneity (45−70 mol % of Bi_2Se_3). The first structural data of this phase were published a few years later, in 1978.[11] Its structure is based on a 21-layer rhombohedral lattice, with a range of existence from 45 to 66.7 mol % of Bi_2Se_3. For the composition 50 mol % of Bi_2Se_3, the hexagonal lattice parameters were $a = 4.188$ Å and $c = 39.46$ Å. To our knowledge, no detailed structural study of this phase has been reported.

According to Odin et al.,[10,11] there are two ranges of solid solution for SnSe-rich and Bi_2Se_3-rich compounds, where the limits of existence depend on the temperature. Thus, for example, at 640 °C, for a given composition of 20 mol % of Bi_2Se_3 (4 SnSe·Bi_2Se_3), a mixture of a SnSe-rich phase plus the 21-layer rhombohedral phase mentioned above is obtained. This mixture corresponds to a global composition $Sn_4Bi_2Se_7$.

On the other hand, we have recently reported a detailed study of the temperature transformations of SnSe.[12] Other group 14 selenides show a NaCl-related structure at high temperature, e.g. GeSe. This is not the case of SnSe, which melts before

† Permanent address: Laboratoire de Chimie Minérale, Faculté de Sciences et Techniques, Université de Cocody, 22 BP 582, Abidjan, Ivory Coast.

(1) Rowe, D. M.; Bhandari, C. M. *Modern Thermoelectrics*; Holt, Rinehart and Winston: London, 1983.
(2) Mishra, S. K.; Satpathy, S.; Jepsen, O. *J. Phys. Cond. Matter* **1997**, *9*, 461−470.
(3) Ettenberg, M. H.; Maddux, J. R.; Taylor, P. J.; Jesser, W. A.; Rosi, F. D. *J. Cryst. Growth* **1997**, *179*, 495−502.
(4) Kulbachinskii, V. A.; Negishi, H.; Sasaki, M.; Giman, Y.; Inoue, M.; Lostak, P.; Horak, J. *Phys. Status Solidi. B. Basic Res.* **1997**, *199*, 505−513.
(5) Yashima, I.; Tsukuda, R.; Sato, T.; Tochio, Y. *J. Ceram. Soc. Jpn.* **1997**, *105*, 1018−1021.
(6) Navratil, J.; Stary, Z.; Plechacek, T. *Mater. Res. Bull.* **1996**, *31*, 1559−1566.
(7) Shafa, C.; Brett, M. J. *Can. J. Phys.* **1996**, *74*, S139−S142.
(8) Hemmerich, J. L.; Loos, J. C.; Miller, A.; Milverton, P. *Rev. Sci. Inst.* **1996**, *67*, 3877−3884.
(9) Hirai, T.; Takeda, Y.; Kurata, K. *J. Less-Common Metals* **1967**, *13*, 352−356.
(10) Odin, I. N.; Gospodinov, G. G.; Novoseleva, A. V.; Sher, A. A. *Vest. MGU, Ser. Khim.* **1974**, *29*, 285−288.
(11) Sher, A. A.; Odin, I. N.; Novoseleva, A. V. *Izv. Akad. Nauk SSSR, Neorg. Mater.* **1978**, *14*, 1270−1276.
(12) Adouby, K.; Pérez Vicente, C.; Jumas, J. C.; Fourcade, R.; Abba Touré, A. *Z. Kristallogr.* **1998**, *213*, 343−349.

10.1021/ic9812858 CCC: $18.00
Published on Web 04/09/1999

Table 1. Summary of Crystallographic Data and Structure Refinement of Bi_2Se_3 and $SnBi_4Se_7$

nominal composition	Bi_2Se_3	$SnBi_4Se_7$
no. of Se layers per slab	3	4
reduced formula per slab	Bi_2Se_3	$Sn_{0.571}Bi_{2.286}Se_4$
MW per reduced formula	654.84	861.34
crystal system	trigonal (hexagonal axes)	trigonal (hexagonal axes)
space group (No.)	*R*3*m* (166)	*R*3*m* (166)
Z per reduced formula	3	3
a (Å)	4.1355(5)	4.1602(5)
c (Å)	28.615(2)	38.934(3)
V (Å^3)	423.6	673.8
D_X (g cm^{-3})	7.702	6.366
$D_{measured}$ (g cm^{-3})	−	6.34
reliability factors		
R_p	0.1219	0.0681
R_{wp}	0.1628	0.0872
$R_{expected}$	0.1091	0.0640
goodness of fit	1.48	1.35
R_{Bragg}	0.0620	0.0500
data collection		
radiation		Cu Kα
wavelength (Kα$_1$, Kα$_2$, Kα$_2$/Kα$_1$ ratio)		1.5404 Å, 1.5443 Å, 0.52
2θ range		12−102°
2θ step		0.02°
recording time/step		20 s

Atomic Position, Occupancy, and Thermal Parameters

atom	site[a]	occupancy	*Z* in (0, 0, *z*) position	thermal parameters[b] *U*(1,1)	*U*(3,3)
			Bi_2Se_3		
Bi	6c	6	0.4006(1)	0.005(3)	0.00069(5)
Se	3a	3	0	0.036(9)	0.0005(2)
Se	6c	6	0.2109(2)	0.016(8)	0.0011(1)
			$SnBi_4Se_7$		
Bi	6c	5.74(2)	0.4285(1)	0.004(3)	0.00017(5)
Sn + Bi	3a	1.17 + 1.12(2)	0	0.014(2)	0.00047(7)
Se	6c	6	0.1350(2)	0.031(8)	0.0004(1)
Se	6c	6	0.7108(2)	0.08(1)	0.00052(7)

[a] 3a (0, 0, 0); 6c (0, 0, *z*). [b] $U(1,1) = U(2,2) = 2U(1,2)$; $U(1,3) = U(2,3) = 0$.

adopting that structure. To obtain the high temperature form, with a NaCl type structure, we have studied the $Sn_{1-3x}Bi_{2x}Se$ series. From these studies, a new phase $Sn_4Bi_2Se_7$ was identified.[12] This new phase has no existence in the phase diagram proposed by Odin et al.[10] Thus, we decided to reexamine the complete phase diagram of the system SnSe−Bi_2Se_3. During this study, a similar phase to the rhombohedral one described above has been obtained, but with a restraint range of existence, close to 67% mol of Bi_2Se_3. Here, we report the structural study of this phase, with nominal composition $SnBi_4Se_7$, based on the results obtained by ^{119}Sn Mössbauer spectroscopy and X-ray diffraction, including Rietveld analysis. The complete phase diagram will be soon published separately.

Experimental Section

The binary tin and bismuth selenides, SnSe and Bi_2Se_3, were prepared by a solid-state reaction from pure elements, while the ternary compound $SnBi_4Se_7$ was prepared from the binary compounds. Stoichiometric mixtures were placed into a silica tube and sealed under vacuum (~10^{-5} Torr). For SnSe and Bi_2Se_3, the mixtures were heated at 30 °C/h up to 800 °C, maintaining this temperature constant for four and 2 days, respectively, and then slowly cooled to room temperature. For $SnBi_4Se_7$ the mixture was heated at 50 °C/h up to 900 °C for 3 days, then slowly cooled to 640 °C and maintained at this temperature for 2 weeks. Finally, the sample was quenched in an ice−water bath.

X-ray powder diffraction (XRD) patterns were alternatively recorded on Philips model and Siemens D5000 diffractometers, using Cu Kα radiation. To minimize preferred orientation phenomena, the preparation of the samples was as follows: the sample holder was covered with a thin adhesive film, and the products were then finely ground and passed through a 5 μm sieve directly on the sample holder. The recordings of the XRD patterns for Rietveld analyses have been carried out under the experimental conditions which are summarized in Table 1. Rietveld analyses were carried out with the aid of the Rietveld analysis program DBWS-9411.[13]

^{119}Sn Mössbauer spectra were recorded in the constant acceleration mode on a ELSCINT-AME40 spectrometer, provided with a cryostat for the measurement at low temperature (up to 4 K). The absorbers were prepared to have 1−2 mg of ^{119}Sn per cm^2. The source of γ-ray was $Ba^{119m}SnO_3$. The velocity scale was calibrated with the magnetic sextet spectrum of a high purity iron foil absorber, using ^{57}Co(Rh) as source. Recorded spectra were fitted to Lorentzian profiles by least-squares method.[14] The origin of the isomer shift was determined from the center of the $BaSnO_3$ spectrum recorded at room temperature.

Results and Discussion

Figure 1 shows the experimental XRD patterns of $SnBi_4Se_7$, where the main reflections have been indexed by using hexagonal unit cell parameters $a = 4.16$ Å and $c = 38.9$ Å. For the *hkl* values, some reflection conditions appear: $l = 3n$ for *00l* reflections and $-h + k + l = 3n$ for general *hkl* reflections. These indicate a rhombohedral-type unit cell. The experimental density of the compound is 6.34 g/cm^3. From these parameters, a noninteger value of *Z* is obtained when using the

(13) Young, R. A.; Sakthivel, A.; Moss, T. S.; Paiva-Santos, C. O. *J. Appl. Crystallogr.* **1995**, *28*, 366.
(14) Künding, W. *Nuclear Inst. Methods* **1969**, *75*, 336−340.

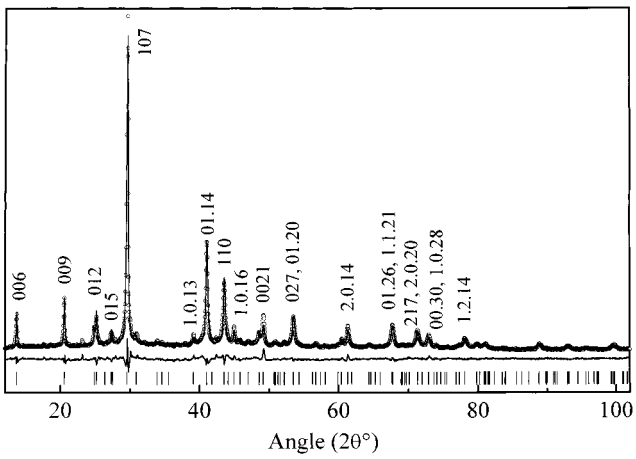

Figure 1. Experimental and refined XRD patterns of $SnBi_4Se_7$ (refined parameters are included in Table 3). The preferred orientation has been avoided (see Experimental Section).

$SnBi_4Se_7$ unit formula. For $Z = 3$, which is the minimum multiplicity of sites in a rhombohedral unit cell expressed in hexagonal axes, an alternative unit formula can be used: $Sn_{0.571}Bi_{2.286}Se_4$.

With the aim of using the structure factors derived directly from the Rietveld analysis in the electron density study of $SnBi_4Se_7$ and to compare it with Bi_2Se_3, XPD data of the latter phase were also used. The results of Rietveld refinement are included in Table 1 and fit well to previously reported structural data.[15] Bi_2Se_3 has a layer trigonal structure (space group $R\bar{3}m$). The unit cell using hexagonal axes is composed of three slabs, where the sequence of atomic layers within each slab is Se−Bi−Se−Bi−Se. The values of the lattice parameter a of $SnBi_4Se_7$ and Bi_2Se_3 are close (4.160 and 4.134 Å, respectively, with a relative difference of 0.6%). It indicates that the presence of Sn atoms in the structure does not modify the packing of Se atoms in $hk0$ planes compared to Bi_2Se_3. Concerning the lattice parameter c, the value for Bi_2Se_3 is 28.615 Å. This value diverges from the ternary, probably indicating strong variations in the atomic sequence from one selenide to the other. In Bi_2Se_3, selenium atoms are placed in 3a (0, 0, 0) and 6c (0, 0, z) sites, with $z = 0.2109$. Taking into account the generator vectors, the Se−Se distances along the c axis can be calculated. Thus, the intralayer Se−Se distances are found to be 3.503 Å, while the interlayer one is 2.531 Å. Assuming that the presence of tin atoms does not modify basically these distances, the theoretical basal spacing of a slab with a Se−Bi−Se−Bi−Se−Bi−Se atomic sequence can be derived as $3 \times 3.503 + 2.531 = 13.04$ Å, and if the unit cell is composed of three slabs, as in the case of Bi_2Se_3, it gives $3 \times 13.04 = 39.12$ Å. The latter value is close to that obtained for $SnBi_4Se_7$, 38.9 Å, where the small difference (of about 0.6%, and similar to that obtained for a) can be attributed to the very slight distortion created by Sn atoms in the S packing, as compared with Bi_2Se_3.

While for Bi atoms in $SnBi_4Se_7$ a similar local environment to that found in Bi_2Se_3 can be assumed, this is not the case for Sn atoms in $SnBi_4Se_7$, when compared to SnSe. Although tin is in a formal oxidation II in the two compounds, and $SnBi_4Se_7$ is obtained from SnSe and Bi_2Se_3, it is not evident if the final compound can be considered as the product of SnSe insertion into a Bi_2Se_3 host matrix, in which tin atoms retain their local environment.[12] An alternative possibility is a solid solution, with a similar environment for both Sn and Bi atoms. To elucidate between these two options, a ^{119}Sn Mössbauer study of SnSe and $SnBi_4Se_7$ has been carried out. The experimental and refined spectra are shown in Figure 2, and the hyperfine parameters are included in Table 2. The spectrum of SnSe consist on a well-resolved and nonsymmetric doublet, in agreement with previously published data.[12] The values of the isomer shift obtained at 77 and 300 K are characteristic of Sn (II), while the presence of a quadrupolar splitting evidences the strong distortion of the coordination polyhedron surrounding Sn atoms. Additionally, the different contribution of each component of the doublet (which is due to a different nuclear transition probabilities from the ground-state $I = {}^1/_2$ to the two excited states at $I = {}^3/_2$) indicates the well-known Goldanskii-Karyagin effect[16] which is due to the vibrational anisotropy of tin atoms. At 77 K the relative contribution of both components of the doublet (53.2% and 46.8%) are closer than at room temperature (58.2 % and 41.8%). This is a logical result since the Goldanskii−Karyagin effect depends on the average of quadratic vibrational displacement of atoms, which decreases as the temperature decreases.

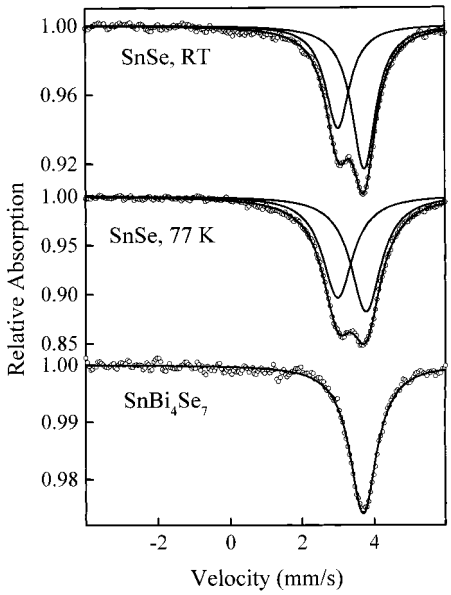

Figure 2. ^{119}Mössbauer spectra of SnSe (recorded at room temperature and at 77 K) and $SnBi_4Se_7$ (recorded at room temperature).

Concerning $SnBi_4Se_7$, the ^{119}Sn Mössbauer spectrum is characterized by the presence of a single nonsplit peak. The value of the isomer shift (3.600 mm/s) indicates again a formal oxidation state Sn(II), which is consistent with an oxidation state assignment of $(Sn^{II})(Bi^{III})_4(Se^{-II})_7$. In addition, the isomer shift value is closer to that observed in $Sn_4Bi_2Se_7$ with NaCl-type structure (3.489 mm/s at 300 K)[12] than for SnSe. The higher value of isomer shift for $SnBi_4Se_7$ can be regarded as a consequence of the increasing ionic character of the Sn−Se bonds. It should be noted that the average of the three shortest Sn−Se distances in SnSe is 2.77 Å, while this average is 2.95 Å in $SnBi_4Se_7$. Thus, we can conclude that Sn atoms present in $SnBi_4Se_7$ are placed in a octahedral coordination, the distortion of the polyhedron being weak enough to be nondetectable in ^{119}Sn spectrum as a quadrupole splitting.

Table 3 contains the indexed list of reflections. For layered rhombohedral compounds, the highest intensity usually corre-

(15) Nakajima, S. *J. Phys. Chem. Solids* **1963**, *24*, 479−485.

(16) Bauminger, E. R.; Nowik, I. The dynamics of nuclei studied by Mössbauer spectroscopy. In *Mössbauer spectroscopy*; Dickson, D. P. E., Berry, F. J., Eds.; Cambridge University Press: Cambridge, UK, 1986.

Table 2. Hyperfine Parameters of ^{119}Sn Mössbauer Spectra of SnSe and $SnBi_4Se_7$: Isomer Shift (IS), Quadrupole Splitting (QS), Line Width (LW), and Contribution of Each Component of the Doublet (case of SnSe)

compound	temperature	IS (mm/s)	QS (mm/s)	LW (mm/s)	contribution C_1 (%)	contribution C_2 (%)
SnSe	300 K	3.269 (8)	0.725 (8)	0.806 (8)	58.2	41.8
	77 K	3.291 (8)	0.784 (8)	1.021 (8)	53.2	46.8
$SnBi_4Se_7$	300 K	3.600 (4)	–	0.91 (1)	–	–

Table 3. List of Observed Reflections and Intensities Present in the XRD Pattern of $SnBi_4Se_7$ (Figure 1)

angle (2θ°)	h	k	l	I/I_0	angle (2θ°)	h	k	l	I/I_0	angle (2θ°)	h	k	l	I/I_0
13.66	0	0	6	92	52.20	1	1	12	7	74.06	1	1	24	17
20.54	0	0	9	113	53.44	0	2	7	158	76.84	2	1	13	12
24.82	1	0	1	41	53.48	0	1	20	10	77.28	2	0	23	16
25.14	0	1	2	93	54.26	2	0	8	4	78.08	1	2	4	101
27.28	0	1	5	43	56.68	1	1	15	7	79.80	0	3	0	50
27.48	0	0	12	11	56.72	0	0	24	8	80.82	2	1	16	20
29.54	1	0	7	1000	58.04	1	0	22	4	81.02	1	0	31	22
30.88	0	1	8	27	59.88	0	2	13	8	81.44	0	3	6	8
33.90	1	0	10	8	60.38	0	1	23	36	83.48	0	3	9	13
39.10	1	0	13	34	61.28	2	0	14	110	87.32	1	2	20	9
40.98	0	1	14	463	64.30	0	2	16	21	88.80	1	1	30	27
43.48	1	1	0	336	67.64	1	1	21	170	88.82	0	2	28	38
44.94	1	0	16	70	68.96	2	1	1	8	92.90	0	1	35	44
45.78	1	1	6	26	69.10	1	2	2	11	93.10	1	2	23	17
46.98	0	1	17	20	70.10	1	2	5	7	95.58	2	2	0	31
48.54	1	1	9	64	71.24	2	1	7	142	96.78	0	2	31	9
49.12	0	0	21	120	71.28	2	0	20	7	97.20	2	2	6	6
50.70	0	2	1	7	71.96	1	2	8	5	99.24	2	2	9	8
50.88	2	0	2	12	72.82	0	0	30	10	99.40	1	0	37	16
52.08	2	0	5	7	72.86	1	0	28	88	99.68	0	3	21	52

sponds to the (01l) reflection (or (10l), according to the reflection condition $-h + k + l = 3n$), where l is the number of the atomic layers in the slab. Since in our case the highest intensity corresponds to the (107) reflection, we can conclude that the basic slab is composed by seven atomic planes. This result is in good agreement with calculations done above, where the lattice parameter c estimated for a unit cell based on three slabs, each one having a sequence of atomic layers Se−Bi−Se−Bi−Se−Bi−Se, was close to that calculated for $SnBi_4Se_7$. This result also confirms the first structural data published on this phase in 1978.[11]

Having in mind all the data discussed above, we tried the refinement of the structure of $SnBi_4Se_7$ on the basis of a layer rhombohedral structure, space group $R\bar{3}m$. Selenium atoms were placed in two different sets of 6c sites, while Sn and Bi where placed in 3a and 6c sites. In a first approach, the metal ions were randomly distributed between both sites. After the first refinement, the occupation factors of Sn and Bi in 3a and 6c sites were also allowed to be refined, keeping constant the global composition of the solid. The final result of the refinement is included in Table 1. Figure 3 schematizes the structure of this compound, where only one Se−M−Se−M−Se−M−Se slab is present, the unit cell being composed of three slabs. It is worth noting that cations are not fully random distributed in the solid. Thus, in site 6c ($z = 0.4285$) only Bi atoms are present (with the presence of 4.3% of vacancies), while in site 3a we find both Sn and Bi atoms (with 5.7% of vacancies).

The one-dimensional electron density plots of Bi_2Se_3 and $SnBi_4Se_7$ along [001] were obtained by the Patterson analysis from the intensity of (00l) reflections up to $l = 30$. The plots for one-third of the unit cell are combined with the projection of the structures in the *ac* plane in Figure 4, from which the close relationship between the slabs of both compounds is clearly visualized. In addition, it is worth noting that the electron density peaks corresponding to selenium atoms in each one of the two nonequivalent sites of each compound differ significantly in

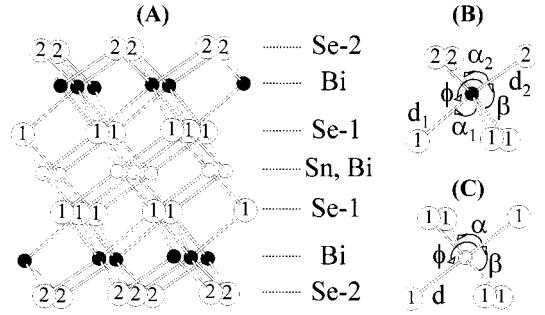

Figure 3. (A) Schematic of the structure of $SnBi_4Se_7$, where only one Se−M−Se−M−Se−M−Se layer is present, the unit cell being composed of three layers. (B) Coordination polyhedron of Bi atoms placed in site 6c. (C) Coordination polyhedron of Bi and Sn atoms placed in site 3a.

broadening. Thus, the signals of 3a Se in Bi_2Se_3 and 6c Se with $z = 0.7108$ in $SnBi_4Se_7$ are particularly broadened, as compared with 6c Se in Bi_2Se_3 and 6c Se with $z = 0.1350$ in $SnBi_4Se_7$. The former selenium atoms are in the inner atomic layer of the slabs and coordinated by metal atoms exclusively. On the contrary, the latter selenium atoms are exposed to the interlayer space, having three short metal−selenium distances and three long selenium−selenium distances affecting the Se atoms in the neighbor slab. As interslab Se−Se interactions are purely van der Waals forces, the electron density in these atoms is confined into a smaller volume than in selenium atoms having exclusively true chemical bonds with the surrounding metal atoms. Further insight on the electron density plots reveals that the van der Waals gap is larger in Bi_2Se_3 as compared with $SnBi_4Se_7$. This is an expected result, as the layered character of the solids decreases with the thickness of the slabs due to the long-range interactions between atoms. Moreover, these divergences are of great value in order to consider chemical properties of these solids, such as intercalation properties.

Figure 3C also shows the coordination polyhedra of both cationic sites. The values of distances and angles of the different

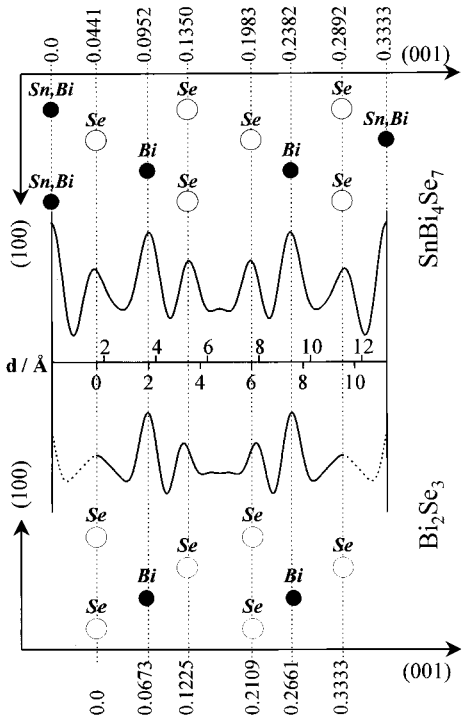

Figure 4. Electron density plots along [001] and projection of the structure of Bi_2Se_3 and $SnBi_4Se_7$ in the *ac* plane. Both diagrams and structures are centered at the van der Waals gap to allow a direct comparison and include one-third of the unit cell, the other two-thirds being equivalent.

Table 4. Distances and Angles in the Polyhedra Coordination of Metallic Atoms of Bi_2Se_3 and $SnBi_4Se_7$ as Defined in Figure 3

	Bi_2Se_3		$SnBi_4Se_7$
	6c	**6c**	**3a**
occupancy	6 Bi	5.74(2) Bi	1.17 Sn + 1.12(2) Bi
d_1 (Å)	3.066(4)	3.117(4)	2.953(4)
d_2 (Å)	2.861(3)	2.859(3)	2.953(4)
Se−Se interlayer	3.479(4)		3.442(4)
α_1 (deg)	84.8(1)	83.7(1)	89.6(1)
α_2 (deg)	92.5(1)	93.4(1)	
β (deg)	91.3(1)	91.3(1)	90.5(1)
ϕ (deg)	174.6(2)	173.3(2)	180.0(2)

polyhedra are included in Table 4. Concerning the site 3a, this polyhedron is an almost perfect regular octahedron, in which the distances to the six selenium are the same. Also, the values of the different angles α and β show that the distortion is negligible. Additionally, the value of $\phi = 180° = \alpha + \beta$ also agrees with the fact that Bi and Sn atoms are placed exactly at the center of the polyhedron (Figure 3B).

Concerning the site 6c, the situation is different. The six neighbors are placed at two different distances (d_1 and d_2 in Table 4) showing and important distortion compared to a perfect regular octahedron. The different angular values, α_1, α_2, and β also evidence this distortion. Additionally, the value of ϕ is different of $\alpha_1 + \beta$ and $\alpha_2 + \beta$, thus showing that Bi atoms are somewhat displaced from the center of the polyhedron. This local environment for Bi atoms is closer to that found in Bi_2Se_3 that the environment of site 3a, as can be observed from data included in Table 4.

The cation distribution described above is also coherent with the ^{119}Sn Mössbauer data. Tin atoms have found to be in a nondistorted octahedral coordination, as it was deduced from the hyperfine parameters of the ^{119}Sn Mössbauer spectra. As an indirect proof, it can be assumed that tin atoms are placed in site 6c. In this case, because of the distortion of the coordination polyhedron, a nonnegligible quadrupolar splitting will be expected, situation which is not observed in the Mössbauer spectrum.

Finally, the structure of $SnBi_4Se_7$ differs from that found for similar compounds. Thus, some bismuth-based tellurides crystallize according to the $P\bar{3}m1$ space group. This is the case, for example, for MBi_4Te_7 (M = Pb, Ge), where the unit cell contains 12 atomic planes, according to the sequence Te−Bi−Te−Ge−Te−Bi−Te...Te−Bi−Te−Bi−Te, after published results of Imanov et al.[17]

Conclusion

First studies of the ternary system $SnSe-Bi_2Se_3$ revealed the existence of a nonstoichiometric trigonal phase with a wide range of existence, from 45% to 66.7% mol of Bi_2Se_3. We have identified and isolated this phase but with a narrow range of existence close to 67% of Bi_2Se_3, corresponding to the composition $SnBi_4Se_7$. The ^{119}Sn Mössbauer spectrum, as compared with those obtained for the orthorhombic phase SnSe and the cubic phase $Sn_4Bi_2Se_7$, allows us to attribute an almost perfect regular octahedral coordination for tin atoms. From the comparison of Se−Se distances to the lattice parameter *c* of $SnBi_4Se_7$, we can conclude that the unit cell is composed of three slabs according to the atomic sequence Se−M−Se−M−Se−M−Se. After Rietveld refinement of XRD patterns according to $R\bar{3}m$ symmetry, the structural parameters of this phase have been determined: $a = 4.1602(5)$ Å and $c = 38.934(3)$ Å. Bismuth atoms partially occupy two sites, 3a (0, 0, 0) and 6c (0, 0, *z*) with $z = 0.4285$, while tin atoms partially occupy only one site, 3a. Selenium atoms are placed in two different 6c sites, with $z_1 = 0.1350$ and $z_2 = 0.7108$.

Acknowledgment. K.A. is indebted to the Ministry of Scientific research of Ivory Coast for financial support. C.P.V. is grateful to the European Community, Training and Mobility of Researchers program (Contract No. ERFFMBICT 98.3020).

IC9812858

(17) Imanov, R. M.; Semiletov, S. A.; Pinsker, Z. G. *Sov. Phys. Crystallogr.* **1970**, *15*, 239−244.